Water Research X 24 (2024) 100257

Contents lists available at ScienceDirect

Water Research X

journal homepage: www.sciencedirect.com/journal/water-research-x

Isotope analysis of nitrogen removal pathways and N_2O production potential in the SDAD-anammox system under different N/S ratios

Mengjia Zhan, Wei Zeng *, Xiaojing Hao, Haohao Miao, Yao Lu, Wenzhuo Jiang, Qingan Meng, Qingteng Gong

National Engineering Laboratory for Advanced Municipal Wastewater Treatment and Reuse Technology, Beijing University of Technology, Beijing 100124, China

ARTICLE INFO

Keywords:
Denitrification desulfurization system
Anammox
Isotope effect
Nitrous oxide
Functional gene

ABSTRACT

This study explored the impact of varying nitrate to sulfide (N/S) ratios on nitrogen removal efficiency (NRE) in the sulfide-driven autotrophic denitrification and anammox (SDAD-anammox) system. Optimal nitrogen removal was observed at N/S ratios between 1.5 and 2.0. Isotope tracing results showed that the contribution of anammox to nitrogen removal was enhanced with increasing N/S ratios, reaching up to 37 % at the N/S ratio of 2.5. Additionally, complex nitrogen pathways were identified, including dissimilatory nitrate reduction to ammonium (DNRA). Furthermore, isotope tracing was innovatively applied to investigate N_2O emissions, demonstrating that higher N/S ratios significantly reduced N_2O emissions, with the lowest emissions at N/S ratio of 2.5. Gene expression analysis indicated that nitrogen and sulfide transformation genes decreased with increasing N/S ratios, while anammox-related genes first increased and then decreased, reflecting the system's microbial dynamics. These findings offer insights into nitrogen transformation pathways and N_2O production mechanisms in the SDAD-anammox process.

Introduction

Anaerobic ammonium oxidation (anammox) has attracted global interest as an efficient and innovative technology for wastewater treatment. Due to the limit of nitrite (NO_2^--N) in wastewater, it is typically combined with partial nitrification (PN) and partial denitrification (PD) for nitrogen removal (Wu et al., 2022a). However, the instability of NO_2^--N generation in PN restricts the widespread application of partial nitrification and anammox (PN/A) (Joss et al., 2009; Bunse et al., 2020). In contrast, coupling of PD with anammox (PD/A) is more feasible because PD can produce stable NO_2^--N and enhance NRE by reducing the nitrate (NO_3^--N) generated by anammox (Du et al., 2022, 2023). The development of PD/A has primarily focused on generating NO_2^--N through heterotrophic partial denitrification, where organic carbon serves as the electron donor. However, the higher growth rates and biomass yield coefficients of heterotrophic denitrifying bacteria (HDB) compared to ammonia-oxidizing bacteria (AnAOB) may lead to excessive growth of heterotrophs, potentially inhibiting anammox activity (Kumar and Lin, 2010; Cao et al., 2013). Among the studies on autotrophic partial denitrification coupled with anammox, SDAD-anammox has garnered attention for its unique advantages. Firstly, AnAOB and sulfur-oxidizing bacteria (SOB) share similar ecological niches and exhibit intersecting growth conditions regarding temperature, pH, etc. (Kuypers et al., 2018; Strous et al., 1999). Studies have confirmed that coexistence of AnAOB and SOB facilitates simultaneous removal of nitrogen and sulfide (S^{2-}) (Kalyuzhnyi et al., 2006; Wu et al., 2020). Secondly, the relatively low biomass of SOB helps alleviate conflicts between AnAOB and SOB (Lu et al., 2018). All evidence suggests that the SDAD-anammox is a promising approach for nitrogen removal.

The ratio of NO_3^--N to S^{2-} (N/S) is crucial to the efficiency of the SDAD-anammox system. Reyes-Avila et al. (2004) reported that at an N/S ratio of 1:1, NO_3^--N was reduced to NO_2^--N and S^{2-} was oxidized to S^0 (Eq. (1)). Theoretically, the N/S ratio should be controlled between 1.0 and 4.0 to achieve higher NO_2^--N conversion (Eq. (1) and Eq. (2)). Qin et al. (2019) found that in the SDAD-anammox system, total nitrogen (TN) removal by anammox could be maintained above 90 % under N/S ratios ranging from 0.96 to 4.56, supporting the theoretical values. However, the most favorable N/S ratio for the anammox reaction remains controversial. Deng et al. (2021) observed that the highest NRE via the anammox (82.8 %) occurred at an N/S ratio of 3.0, while Wu

* Corresponding author at: Department of Environmental Engineering, Beijing University of Technology, Pingleyuan No.100, Chaoyang District, Beijing 100124, China.
E-mail address: zengwei@bjut.edu.cn (W. Zeng).

https://doi.org/10.1016/j.wroa.2024.100257
Received 21 July 2024; Received in revised form 10 September 2024; Accepted 11 September 2024
Available online 11 September 2024

et al. (2020) achieved the highest ammonium conversion rate at N/S ratios of 1.8–2.0. Considering the competition between AnAOB and SOB for NO_2^--N, thermodynamically, the NO_2^--N reduction process driven by S^{2-}/S^0 is more favorable than anammox (Huo et al., 2022). However, AnAOB can induce higher NO_2^--N affinity by virtue of its unique NO_2^--N transporter protein and anammoxosome membrane, making them more competitive than SOB for NO_2^--N under limited supply conditions (van Niftrik and Jetten, 2012). Consequently, the interaction details between anammox and SDAD under varying N/S conditions remain unclear.

$$S^{2-} + NO_3^- + H_2O \rightarrow S^0 + NO_2^- + 2OH^- \quad (1)$$

$$S^{2-} + 4NO_3^- \rightarrow 4NO_2^- + SO_4^{2-} \quad (2)$$

Greenhouse gases produced during the urban wastewater treatment contribute to the carbon footprint of water utilities, preventing the achievement of carbon-neutral (Zhang et al., 2022). Among these gases, N_2O has attracted wide attention due to its high global warming potential (273 times that of CO_2) (Chen et al., 2020). Previous studies have mostly focused on exploring N_2O emissions under different conditions in the SDAD-anammox system (Polizzi et al., 2022; Qian et al., 2018). In fact, N_2O emissions result from the activities of denitrifying bacteria as N_2O sources and bacteria possessing N_2O reductase (NOS) as N_2O sinks.

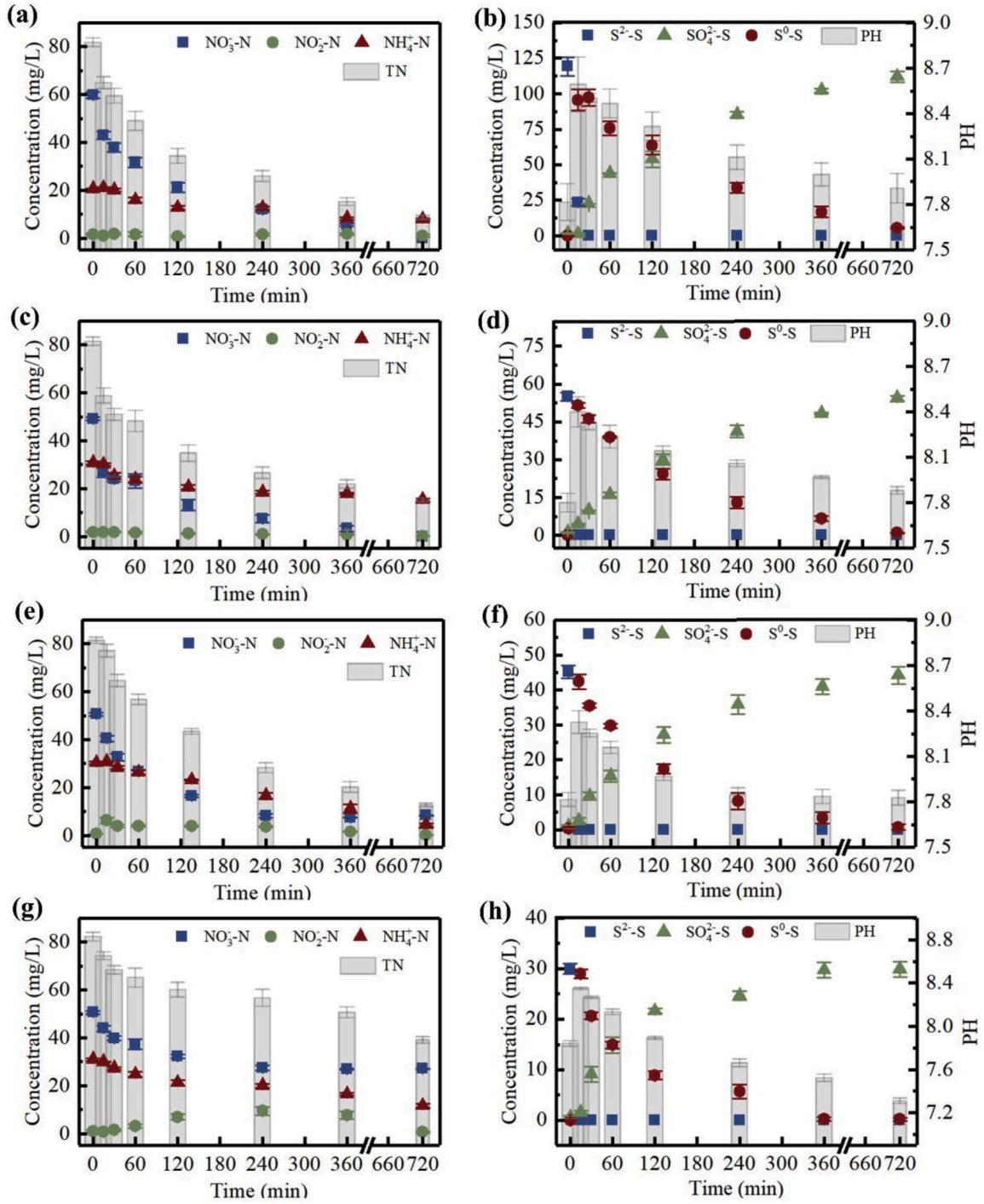

Fig. 1. S^{2-}, NO_3^--N and NH_4^+-N removal and pH variation in typical cycles at the different N/S ratios (a, b: N/S ratio = 1.0; c, d: N/S ratio = 2.0; e, f: N/S ratio = 2.5; g, h: N/S ratio = 4.0).

Therefore, quantifying N_2O production and consumption rates and their response to environmental variables can help develop strategies to reduce N_2O emissions.

This study investigated the performance and mechanism of the SDAD-anammox system under different N/S ratios using activated sludge from a system stably operated for 120 days. The isotope tracing technique was employed to assess the nitrogen removal pathways and N_2O production and consumption activities. By combining the transcriptional activity of relevant functional genes involved in N and S cycling, this study aimed to elucidate nitrogen removal capacity and N_2O production potential in the SDAD-anammox system at different N/S ratios.

Results and discussion

Analysis of nutrient removal characteristics at the different N/S ratios

At a consistent influent TN concentration, the total nitrogen removal rate (TNRR) of the SDAD-anammox process (0.06–0.1 mg/(L min)) was significantly lower than that of the SDAD process (0.18 mg/(L min)) (Figs. 1 and S1). This was attributed to the thermodynamic advantage of SDAD over anammox. In the SDAD-anammox system (Fig. 1), the NRE decreased from 89.09 % to 52.42 % as the N/S ratio increased from 1.0 to 4.0, which was attributed to the insufficient sulfur-related electron donors (S^{2-}/S^0). This was consistent with previous studies (Dolejs et al., 2015; Chen et al., 2018), where the complete SDAD process occurred at N/S less than 1.5. NO_3^--N and NO_2^--N were undetectable in the effluent at N/S ratios of 1.0 and 2.0 (Fig. 1a and c). Notably, the ammonia removal rate (ARR) at N/S ratio of 2.0 (0.029 mg/(L min)) was 1.7 times higher than that at 1.0 (0.017 mg/(L min)), indicating that SDAD predominated at 1.0, while SDAD-anammox dominated at 2.0. As the N/S ratio increased to 2.5 (Fig. 1e), the NRE decreased to 83.4 %, while the ammonium removal efficiency (ARE) further increased to 83 %. A peak in NO_2^--N concentration (6.2 mg/L) was observed at 15 min, confirming the conversion of NO_3^--N to NO_2^--N due to electron acceptor limitation. This is consistent with previous findings (Qin et al., 2019; Wu et al., 2020), which indicated that an N/S ratio of 2.0–2.5 was favorable for the SDAD-anammox process. As the N/S ratio further increased to 4.0 (Fig. 1g), both NRE and ARE decreased to 46 % and 62 %, respectively. Only part of NO_3^--N was converted to NO_2^--N due to the severe lack of S^{2-} as electron donor, resulting in decreased NRE.

Sulfide removal efficiency (SRE) reached 100 % in all conditions (Fig. 1b, d, f and h). Trace amount of S^0 (5 mg/L) was detected in the effluent at the N/S ratio of 1.0 (Fig. 1b), whereas S^{2-} was oxidized to SO_4^{2-} at N/S ratios of 2.0–4.0 (Fig. 1d, f and h), indicating that N/S ratios determined the sulfide reduction products in SDAD-anammox. Additionally, sulfide was rapidly exhausted within 15–30 min. Compared to soluble S^{2-}, the low solubility of S^0 greatly limited its electron-donating capacity (Xu et al., 2014), consequently reducing the NO_3^--N reduction rate. After sulfide exhausted, the accumulation of S^0 peaked. It was hypothesized that sulfide was utilized in two steps: initially, S^{2-} was oxidized to S^0, and then S^0 was further oxidized to SO_4^{2-}. This has been widely confirmed in previous studies (Lee and Wong, 2014; Deng et al., 2021). Additionally, some studies (Fu et al., 2023; Liu et al., 2017) suggested that during the conversion of S^{2-} to S^0, NO_3^--N was preferentially converted to NO_2^--N. This study showed a different viewpoint, i.e., whether NO_3^--N was first converted to NO_2^--N depended on the N/S ratio, since the accumulation of NO_2^--N was found only at N/S ratios of 2.5 and 4.0 (Fig. 1e and g). Since the S^{2-} concentrations at N/S ratios of 2.5 and 4.0 were lower than those at 1.0 and 2.0 (Table 1), it was believed that the NO_2^--N accumulation was unrelated to the inhibitory effect of S^{2-} on AnAOB.

The pH value initially rose and then declined, reaching its peak when sulfide was completely depleted (Fig. 1b, d, f and h). This phenomenon was due to the consumption of protons during the oxidation of S^{2-} to S^0, followed by proton generation as S^0 oxidized further to SO_4^{2-}.

Table 1
Experimental conditions for the batch tests.

Run	Concentration (mg/L)			N/S (moles/moles)
	NO_3^--N	NH_4^+-N	S^{2-}	
I	80		120	1.5
II	60	20	125	1.0
III	50	30	58	2.0
IV	50	30	45	2.5
V	50	30	30	4.0

Furthermore, as the N/S ratio increased from 1.0 to 4.0, the effluent pH value gradually decreased from 7.91 to 7.31. In the SDAD process, the consumption of 1.0 mol of sulfide required an additional 1.6 mol of protons (Xu et al., 2016), leading to an increase in effluent pH. As the N/S ratio increased, the sulfide concentration decreased, which reduced the proton consumption and consequently lowered the effluent pH.

Nitrogen transformation and contribution of anammox and SDAD to nitrogen removal

The isotope tracing technology revealed the contribution of SDAD and anammox to nitrogen removal (Fig. 2). The N_2 was not detected in the blank control group, which implied that O_2 and NO_x^- were completely consumed. The maximum N_2 production was detected within 480 min at N/S ratio of 1.0 (Fig. 2c) and within 720 min at N/S ratio of 2.5 (Fig. 2g), suggesting that sufficient sulfide accelerates NRE. With calculation of $^{28}N_2$, $^{29}N_2$ and $^{30}N_2$, the amount of N_2 produced by denitrification and anammox at different time points was analyzed. The maximum denitrification rate at an N/S ratio of 1.0 (1.62 umol N_2/min) was higher than that at an N/S of 2.5 (0.76 umol N_2/min). Lower N/S ratios provided a richer supply of electron donors, leading to higher denitrification rates. Denitrification rates peaked earlier at an N/S ratio of 1.0 compared to 2.5. The increase in substrate concentration was attributed to the increase in reaction affinity, which accelerated the denitrification process. This finding has been confirmed by Polizzi et al. (2022). Within 240 min, 42–45 umol of N_2 was produced via the anammox at N/S of 1.0 and 2.5, but the anammox rate at an N/S ratio of 2.5 (0.09 umol N_2/min) was significantly higher than that at N/S of 1.0 (0.03 umol N_2/min) in the subsequent reaction (Fig. 2b and f). This was mainly due to that insufficient S^{2-} reduced the SDAD rate and enhanced anammox pathway at N/S ratio of 2.5.

When the N/S ratio was 1.0, the SDAD process was the main nitrogen removal pathway with a contribution of more than 85 % (Fig. 2d). It is noteworthy that the contribution of anammox to nitrogen removal averaged 11.7 % over 120 min, which was slightly lower than the average contribution of 14.6 % from 120 to 720 min. It may be caused by the slight inhibition of AnAOB by S^{2-} at the beginning of the reaction. The average contribution of anammox to nitrogen removal reached 36.1 % at an N/S ratio of 2.5 (Fig. 2h). In particular, it was as high as 52 % within the first 30 min, showing its remarkable activity. However, no NH_4^+-N degradation was observed within 30 min in the batch experimental (Fig. 1e). It was hypothesized that sulfide-induced reduction of NO_3^--N to NH_4^+-N (DNRA) occurred at the beginning of the reaction leading to an increase in NH_4^+-N concentration, which made up for the decrease in NH_4^+-N concentration caused by anammox. The ability of sulfide to contribute to the DNRA has been widely found in lakes, oceans, and wetlands (Huang et al., 2024; Brunet and GarciaGil, 1996).

N_2O emissions at the different N/S ratios

The isotopes of N_2O ($^{45}N_2O$ and $^{46}N_2O$) changed noticeably throughout the reaction (Fig. 3). $^{46}N_2O$ ($^{15}N^{15}N^{16}O$) consistently emerged as the dominant product, while $^{45}N_2O$ ($^{14}N^{15}N^{16}O$) was virtually absent, indicating that N_2O was primarily produced through denitrification in the SDAD-anammox system (Fig. 3f). Notably, trace

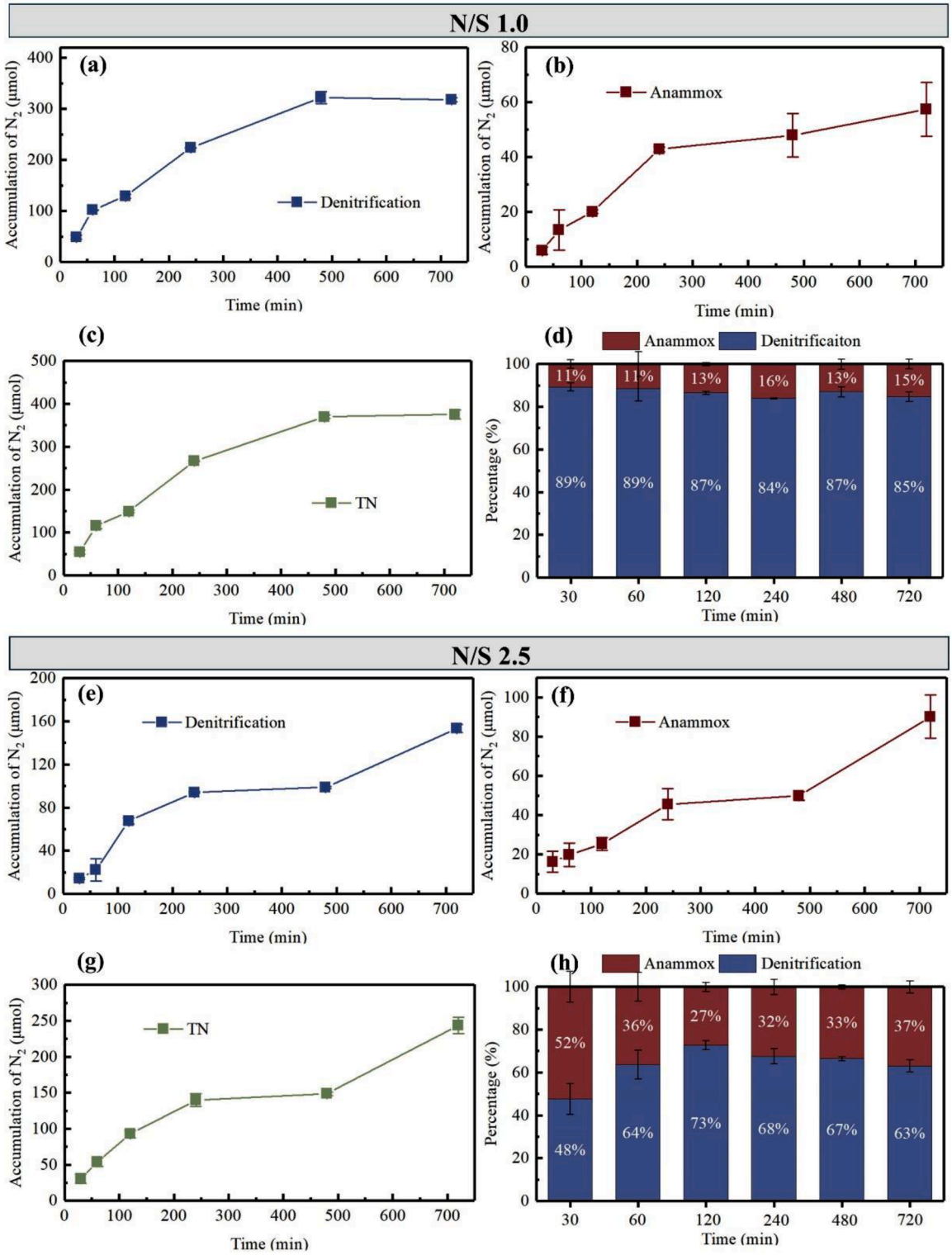

Fig. 2. Isotope analysis of the accumulation of N_2 and the contribution of anammox and SDAD to nitrogen removal (a, b, c, d: N/S ratio = 1.0; e, f, g, h: N/S ratio = 2.5).

amounts of $^{45}N_2O$ were detected at the end of the reaction, suggesting that $^{14}NH_4^+$ had participated in the synthesis of $^{45}N_2O$. Given the substantial production of sulfate from the SDAD observed in this study, it is inferred that a sulfate-induced ammonium oxidation (SRAO) process might have oxidized a small amount of $^{14}NH_4^+$ to $^{14}NO_X^-$, which then combined with the existing $^{15}NO_2^-$ in the system to produce $^{45}N_2O$ (Derwis et al., 2024).

As the reaction progressed, $^{46}N2O$ initially increased and then decreased (Fig. 3a–d). The N_2O emissions in the SDAD-anammox and SDAD accounted for 0.22–1.13 % and 3.78 % of nitrogen loss, respectively (Fig. 3e), demonstrating that SDAD-anammox is more effective in reducing N_2O emissions compared to SDAD. In the SDAD-anammox system, N_2O emissions decreased progressively with increasing N/S ratios (Fig. 3e). The increased N/S ratio led to higher anammox efficiency

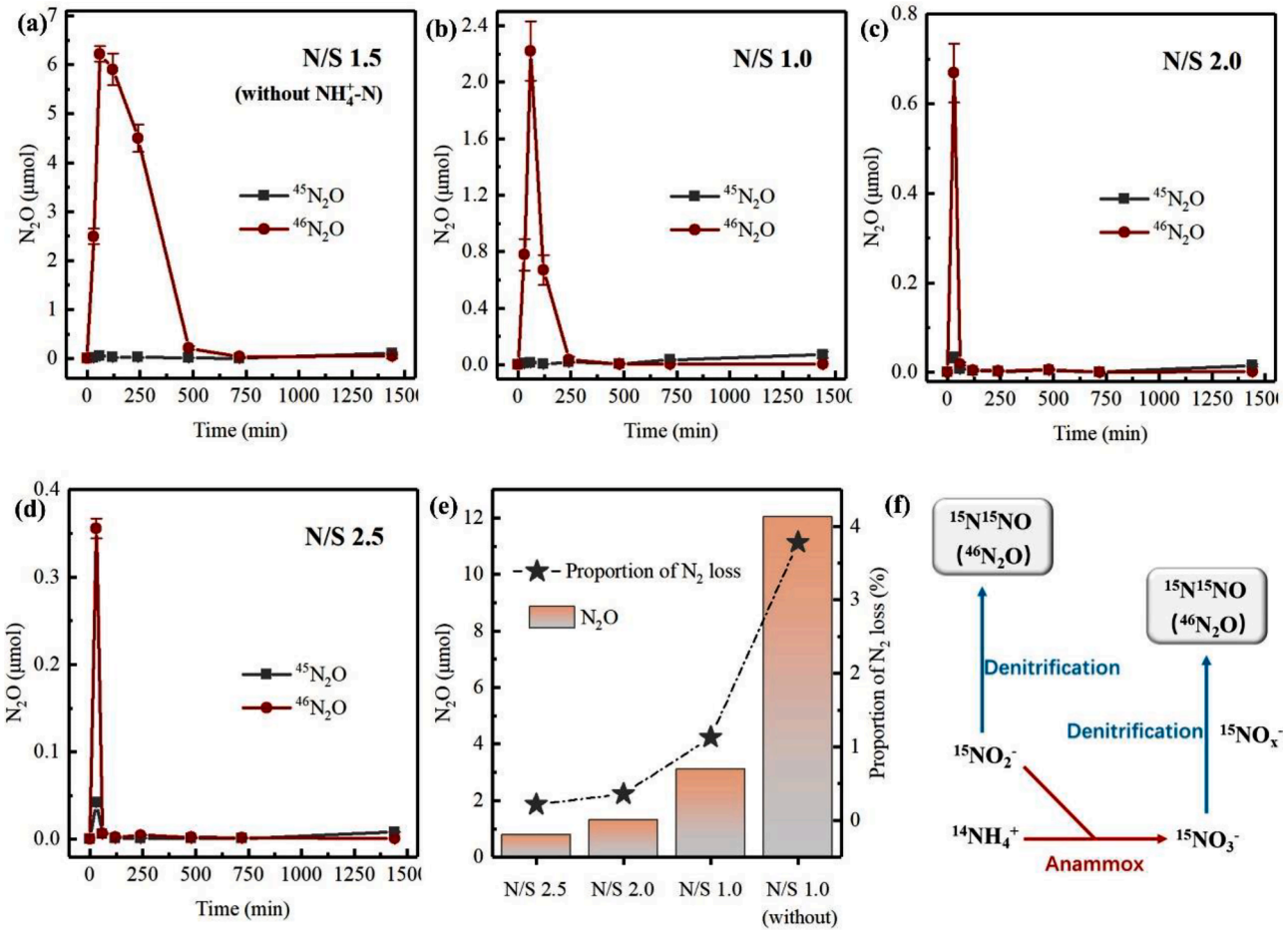

Fig. 3. Variations in N_2O values (a: N/S ratio = 1.5 (without NH_4^+-N); b: N/S ratio = 1.0; c: N/S ratio = 2.0; d: N/S ratio = 2.5), percentage of N_2O emissions (e) and N_2O production pathways (f) in the isotope experiment.

(Fig 2), which in turn resulted in reduced N_2O emissions. Besides, lower N/S ratios corresponded to higher sulfide concentrations, which inhibited the expression of the *nos*Z gene. The inhibitory effect of sulfide on *nos*Z gene expression has been widely documented (Fortune et al., 2024; Martínez-Santos et al., 2018).

^{15}N tracer test to detect N_2O production activity

As an intermediate product of the denitrification pathway, N_2O emissions ($D_{N2Ototal}$) were determined by the N_2O production ($r_{N2Oprod}$) and N_2O consumption ($r_{N2Ocons}$) (Fig. 4a). The ratio of N_2O consumption to N_2O production ($r_{N2Ocons}/r_{N2Oprod}$) was 0.99, 0.99, 0.98, and 0.95 at N/S ratios of 2.5, 2.0, 1.0, and 1.5 (without NH_4^+-N addition), respectively. As the N/S ratio increased, the $r_{N2Ocons}/r_{N2Oprod}$ ratio gradually approached 1.0, indicating a balance between N_2O production and consumption, which in turn led to reduced N_2O emissions.

The production of N_2O comprised both the existing N_2O and the N_2O that had already been converted to N_2 (Fig. 4a). ^{15}N tracer technology helped us reduce errors in the traditional N_2O production calculation method (Suenaga et al., 2021; Ali et al., 2016) and calculate the real N_2O production ($r_{N2O,\ prod}$) in the SDAD-anammox system (Text. S3). The significant relationship between N_2O yield and reaction time could be well described by a Logit model (Fig. 4b–e). N_2O_{max} represented the maximum N_2O production capacity, which was 284.28, 258.59, 247.51, and 240.63 μmol at N/S ratios of 1.5 (without NH_4^+-N addition), 1.0, 2.0 and 2.5, respectively. Lower N_2O_{max} values indicated a reduced capacity for N_2O production, which was beneficial for minimizing N_2O emissions. The λ value represented the N_2O production ratio. As the N/S ratio increased from 1.0 to 2.5, λ decreased from 0.024 to 0.006, suggesting that sufficient sulfide accelerated the gene expression related to the conversion of NO_2^--N to N_2O. Additionally, when the N/S ratio was 1.5 (without NH_4^+-N addition), the λ value for N_2O (0.012) was lower than at an N/S ratio of 1.0 (0.024). Since at N/S ratio of 1.0, the generated NO_2^--N could be used in time through the anammox process, thus avoiding the accumulation of NO_2^--N to inhibit the conversion of NO_2^--N to N_2O.

Quantitative expression of functional genes at the different N/S ratios

The functional gene activities of nitrogen and sulfide metabolic pathways in the SDAD-anammox systems at different N/S ratios were investigated (Fig. 5). In the SDAD-anammox system, the abundance of *nap*A ($NO_3^-\rightarrow NO_2^-$) and *nir*S ($NO_2^-\rightarrow NO$) genes decreased as the N/S ratio increased (Fig. 5a and b). This decline can be attributed to insufficient electron acceptors at higher N/S ratios, leading to reduced denitrification efficiency. The ratio of abundance of nitrate reductase genes and nitrite reductase genes was often used to evaluate the NO_2^--N accumulation capacity of the system (Wu et al., 2022a,b; Liu et al., 2023). At N/S ratios of 2.5 and 4.0, the *nap*A/*nir*S values were 21.1 and 14.4, respectively, significantly higher than those at N/S ratios of 1.0 (3.78) and 2.0 (7.56). This explained the NO_2^--N accumulation observed at N/S ratios of 2.5 and 4.0 (Fig. 1). *Nos*Z, which reduces N_2O to N_2, had expression levels that were closely related to N_2O emissions (Jones et al., 2008). The highest expression level of *Nos*Z was observed at an N/S ratio of 2.5 (7.49×10^6 copies/g sludge), indicating the fastest N_2O reduction rate under this condition (Fig. 5c). This was consistent with the observed

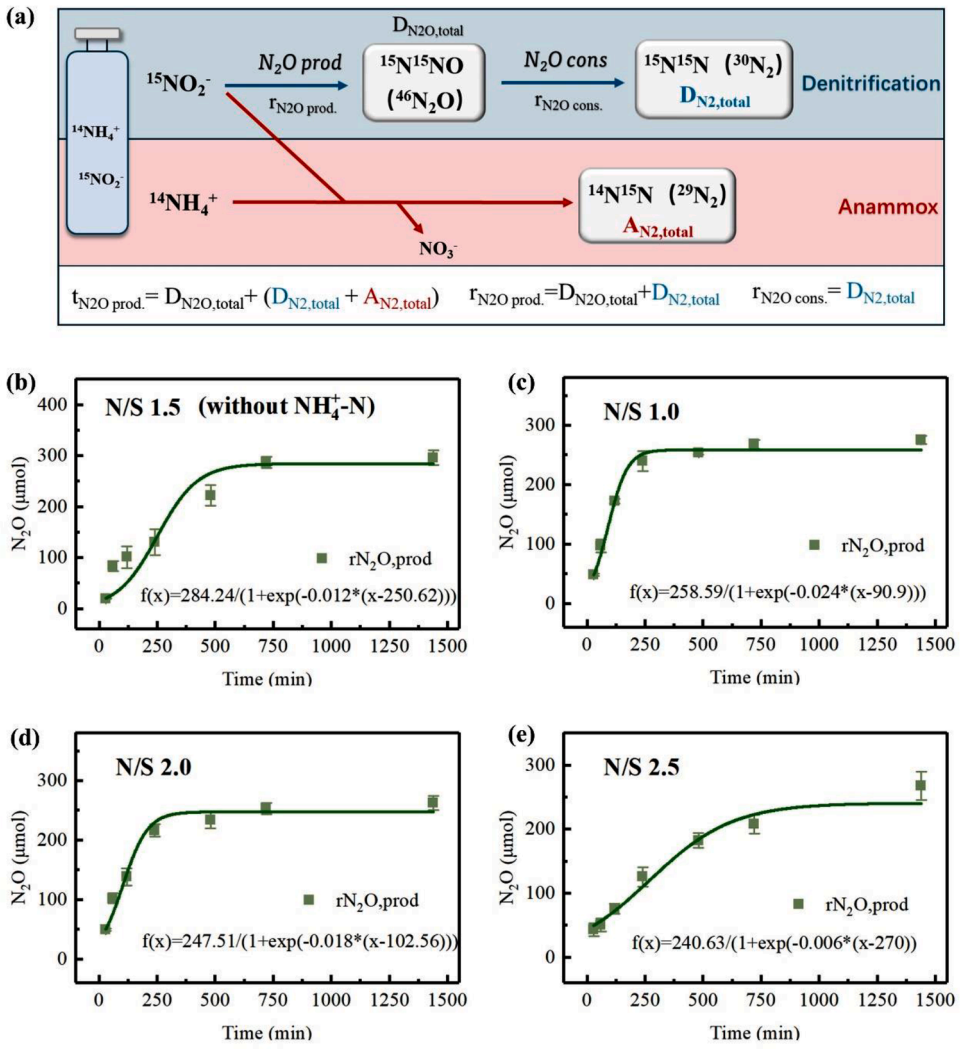

Fig. 4. N_2O production and consumption pathways (a) and the kinetic characteristic of N_2O production (b: N/S ratio = 1.5 (without NH_4^+-N); c: N/S ratio = 1.0; d: N/S ratio = 2.0; e: N/S ratio = 2.5) in the isotope experiment.

N_2O peak being lower at an N/S ratio of 2.5 than that at 1.0 and 2.0 (Fig. 3), confirming that sulfide inhibited the expression of *nos*Z.

As a representative functional gene of anammox, *hzs*B expression levels increased from 1.5×10^5 copies/g sludge to 5.2×10^5 copies/g sludge with increasing N/S ratios (Fig. 5d). This was due to the enhancement of partial denitrification, leading to NO_2^--N accumulation, which is a substrate for anammox. However, at N/S ratio of 4.0, *hzs*B expression decreased to 2.87×10^5 copies/g sludge. Although partial denitrification had an advantage under this condition, the overall denitrification efficiency was significantly reduced, leading to decreased anammox activity.

Sqr and *soxb* are functional genes associated with sulfide transformation, where *sqr* converts S^{2-} into S^0, and *soxb* further converts S^0 into SO_4^{2-} (Luo et al., 2011). In the SDAD-anammox system, the expression levels of both *sqr* and *soxb* decreased with increasing N/S ratios (Fig. 4e and f). This was due to the reduced sulfide concentration, leading to a subsequent decrease in their expression levels. Whether the final sulfur product existed in the form of S^0 or SO_4^{2-} depended on the *sqr*/*soxb* ratio, with a higher *sqr*/*soxb* ratio favoring the accumulation of S^0 (Shi et al., 2024). At the N/S ratio of 1.0, the *sqr*/*soxb* ratio was 1.02, higher than other conditions, which explained why trace amounts of S^0 were detected in the effluent only under this condition.

Additionally, in the SDAD system (without NH_4^+-N addition), the expression levels of *nir*S, *nap*A, and *nos*Z were slightly lower than those in the SDAD-anammox system at an N/S ratio of 1.0, even though the N/S 1.5 system had higher NRE. This suggested that the anammox reaction could enhance the activity of denitrifying bacteria to some extent, possibly by reducing the accumulation of NO_2^--N, which otherwise would inhibit the activity of denitrifying bacteria.

Conclusions

This study demonstrated that the N/S ratio significantly influenced the nitrogen and sulfide removal efficiency in the SDAD-anammox system. Optimal NRE was achieved at the N/S ratio between 1.5 and 2.0. Sulfide limitations affected overall removal efficiency at N/S ratios greater than 2.5. The lowest N_2O emissions occurred at N/S ratio of 2.5 due to enhanced anammox activity. Gene expression analysis of the *hzs*B gene supported these findings, showing increased anammox activity at optimal N/S ratios. To balance efficiency and N_2O emissions reduction, the N/S ratio of 2.5 was recommended, as it maintained 83 % NRE while minimizing N_2O emissions.

Materials and methods

Characteristic of the parent reactor

Typical SDAD-anammox sludge was chosen for batch experiments in

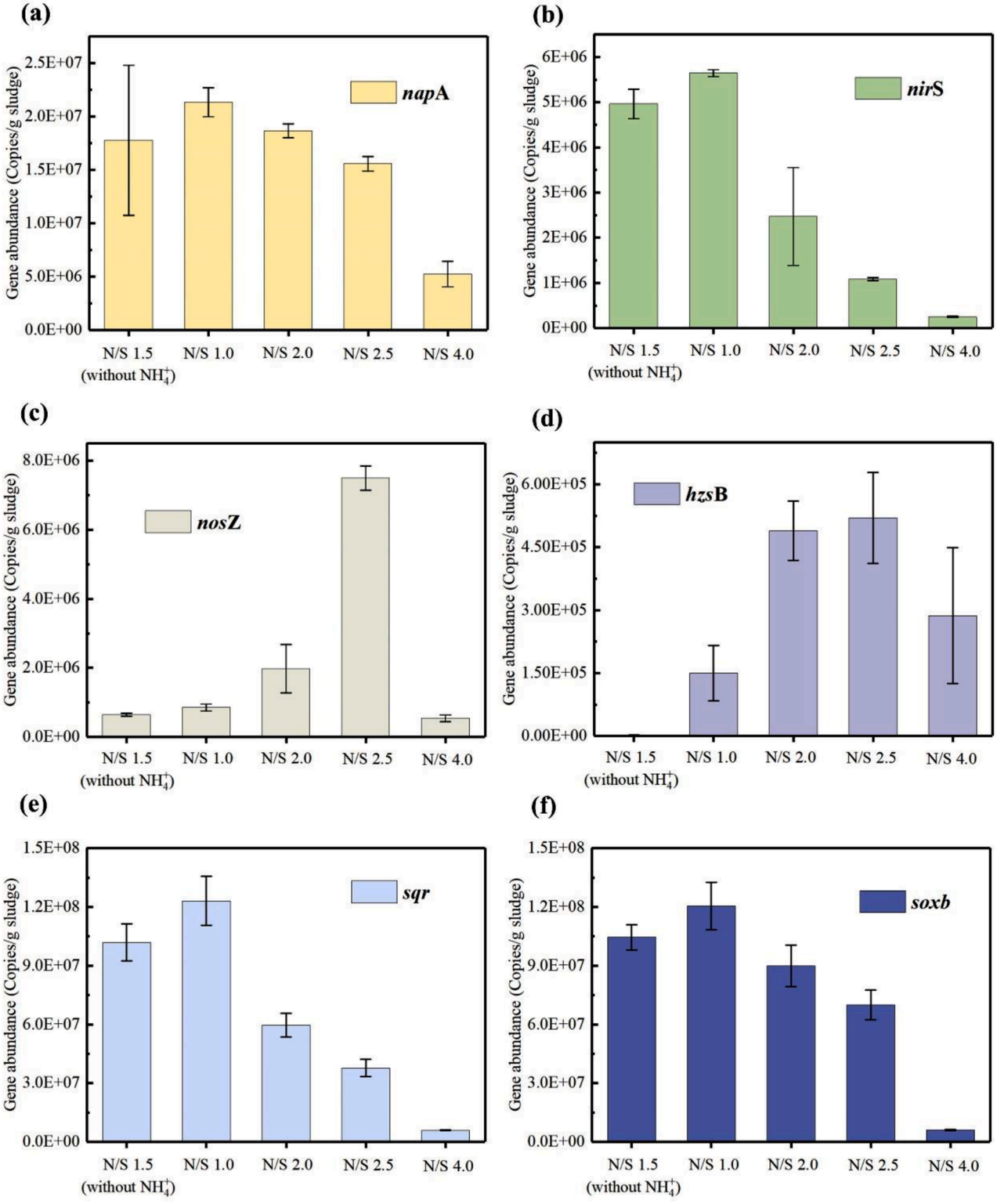

Fig. 5. Abundance of the functional genes related to nitrogen reduction and sulfide oxidation under the conditions of N/S ratios of 1.5 (without NH_4^+-N), 1.0, 2.0, 2.5 and 4.0.

this study. The SDAD-anammox sludge was collected from a parent sequencing batch reactor (SBR). The parent SBR was fed with synthetic wastewater containing 70 mg/L NH_4^+-N, 110 mg/L NO_3^--N and 100 mg/L S^{2-}, where NH_4^+-N from ammonium chloride (NH_4Cl), NO_3^--N from sodium nitrate ($NaNO_3$), and S^{2-} from sodium sulfide nonahydrate ($Na_2S{\cdot}9H_2O$). It was operated at 12 h hydraulic retention time (HRT) for more than 120 days steadily, with NRE as high as 89.7 % and specific anammox activity (SAA) of 2.42 mg NH_4^+-N/ (g VSS h). The other components of synthetic wastewater were: $NaHCO_3$, 1.0 g/L; KH_2PO_4, 0.027 g/L; $CaCl_2{\cdot}2H_2O$, 0.2 g/L; $MgSO_4{\cdot}7H_2O$, 0.3 g/L. Trace element I and trace element II were each 1.0 ml/L (Qin et al., 2019). NaOH/HCl (1 mol/L) was used to maintain an influent pH of 8.0 ± 0.3.

Batch tests

To assess the effect of N/S ratios on the SDAD-anammox process, five serum bottles with an effective volume of 0.5 L were operated in a shaking incubator at 30 ± 1 °C and 200 rpm for batch assays. The inoculums were sampled from the parent reactor and washed twice with distilled water to remove residual substrate. The initial biomass concentration in the serum bottles was approximately 2.12 g VSS L^{-1}. The serum bottles were purged with He gas for 15 min and then injected with sterile anaerobic stock solution. The initial pH was controlled at 8.0 ± 0.3 by NaOH/HCl (1 mol/L).

Five sets of batch assays were conducted under different N/S conditions (1.0, 1.5, 2.0, 2.5, and 4.0), with each condition tested in triplicate to ensure accuracy. The detailed assay design is shown in Table 1. For all conditions, the initial total nitrogen concentration was set at 80 mg/L. Notably, no NH_4^+-N was added under the N/S ratio of 1.5 to compare SDAD and SDAD-Anammox nitrogen removal pathways. Mixed liquor samples were collected periodically until the sulfur was consumed, then these samples were filtered for chemical analyses.

Analytical methods

The collected liquid samples were filtered through a 0.45 μm Millipore filter. The concentrations of NO_3^- - N, NO_2^- - N and NH_4^+ - N were measured according to the standard methods (APHA, 2012). SO_4^{2-} and $S_2O_3^{2-}$ were measured by ion chromatography (Metrosep A Supp 5–250/4.0). The concentrations of H_2S, HS^{-1} and S^{2-} were determined using the methylene blue method (APHA, 2005). The 3420 Multi Parameter Meter (WTW Company, Germany) was to monitor DO and pH on-line. N_2O and N_2 were quantitatively analyzed by isotope mass spectrometer (253Plus, Thermo, United States). S^0 was analyzed according to the method descried by Seth et al. (1995).

Identification of nitrogen conversion pathways by isotopic tracer incubations

^{15}N isotope labeling experiments were conducted to investigate the individual contributions and activity changes of anammox and SDAD in the nitrogen removal process. $Na^{15}NO_3$ (>99.1 %^{15}N, CIL, USA) and $^{14}NH_4Cl$ were used as reaction substrates to evaluate the progress of anammox and SDAD reactions and their contribution to nitrogen removal. Different concentrations of S^{2-} were added to achieve N/S ratios of 1.0 and 2.5 (Table S1). Additionally, a blank control group was set up to determine whether native oxygen (O_2) and NO_x^- (i.e., NO_2^- and NO_3^-) were completely removed during the pre-incubation process. Three parallel tests were set up for each group to ensure the reliability of the results. The specific experimental procedures were as follows: Prior to cultivation, the activated sludge was washed three times with distilled water and pre-incubated anoxically at 30 °C in the dark for 24 h to remove O_2 and NOx^-. The pretreated sludge was divided equally into 2 mL each and placed into 20 mL headspace bottles. Deionized water containing nutrients was then added, and the bottles were purged with high purity He for more than 15 min. The headspace bottles were sealed with butyl rubber stoppers and crimped with aluminum caps. Cultivation was conducted at 30 ± 1 °C for 12 h, followed by the addition of $ZnCl_2$ (0.1 mL, 7 M) to stop microbial activity. The sludge-water mixture of 4 mL was transferred from each sample into a 12 mL sealed vial that has been thoroughly purged with high purity He. Then, the produced $^{29}N_2$ and $^{30}N_2$ were quantified using isotope ratio mass spectrometers (253Plus, Thermo, United States). Calculations of $^{29}N_2$ and $^{30}N_2$ produced by anammox and SDAD were provided in the supplementary material (Text S1 and Text S2).

Determination of N_2O production pathways and rates by ^{15}N tracer tests

^{15}N tracer tests using $Na^{15}NO_3$ (>99.1 %^{15}N, CIL, USA) and $^{14}NH_4Cl$ were performed to determine the pathways of N_2O production, as well as its production and consumption rates at different N/S ratios (Table S2). The specific experimental procedure for the labeling test was consistent with the nitrogen conversion pathway determination experiment. At the end of the incubation, 8 mL of the sludge-water mixture was withdrawn from each sample and equally transferred to two He-purged 12 mL headspace vials. One headspace vial was used directly to determine the N_2 isotope ($^{29}N_2$ and $^{30}N_2$), while the other was placed in a shaker for 30 min to transfer N_2O from the solution into the headspace. Then, 1 mL of headspace gas was withdrawn into 20 mL He-purged headspace vials for the determination of the N_2O isotope ($^{44}N_2O$, $^{45}N_2O$, and $^{46}N_2O$). The concentrations of N_2O isotope ($^{44}N_2O$, $^{45}N_2O$, and $^{46}N_2O$) and N_2 isotope ($^{29}N_2$ and $^{30}N_2$) were determined using isotope ratio mass spectrometers (253Plus, Thermo, United States).

The total accumulated N_2O ($D_{total,\ N2O}$) was the sum of all N_2O isotope, which included $^{14}N^{14}NO$ ($^{44}N_2O$), $^{15}N^{14}NO + {}^{14}N^{15}NO$ ($^{45}N_2O$), and $^{15}N^{15}NO$ ($^{46}N_2O$) (Eq (3)). The true N_2O production ($r_{N2O,\ prod}$) was calculated by (Eq (4)). The $^{30}N_2$ production resulted from $^{46}N_2O$ consumption; therefore, the sum of the N_2O production ($D_{N2O,\ total}$) and $^{30}N_2$ production ($D_{N2,\ total}$) represented the true N_2O production. The calculations for $^{30}N_2$ production ($D_{N2,\ total}$) were provided in the supplementary material (Text S1 and Text S2).

$$D_{total,\ N2O} = D_{44N2O} + D_{45N2O} + D_{46N2O} \quad (3)$$

$$r_{N2O,\ prod} = D_{N2,\ total} + D_{N2O,\ total} \quad (4)$$

Kinetic analysis of N_2O production

The kinetic analysis of the $r_{N2O,\ prod}$ of the system was carried out to understand the N_2O production pattern at different N/S ratios. The Logistic model was used to analyze the generation of new organisms in typical cycles (Zhan et al., 2024). The kinetic models and parameters are as follows:

The Logistic model:

$$N_2O_{prod} = \frac{N_2O_{max}}{1 + \exp\left(-\lambda * (x - x_a)\right)}$$

where N_2O_{prod} represents N_2O production value (μmol). N_2O_{max} represents maximum N_2O production value (μmol), λ represents N_2O production rate (μmol/min), and x_a is the time corresponding to 50 % of maximum N_2O production value (min).

Quantitative reverse transcription PCR (qRT-PCR) of functional genes

To investigate the transcriptional responses of functional genes related to nitrogen (*nap*A, *nir*S, *nos*Z, *hzs*B) and sulfide (*sqr* and *soxb*) transformation under different N/S conditions, 5 mL of mixed liquor was taken from the batch reactors at the end of the batch experiment, and then centrifuged to remove the supernatant. The sludge pellets were immediately stored at −80 °C until use. Total RNA was extracted using the RNA PowerSoil™ Total RNA Isolation Kit (MoBio Laboratories Inc, USA). RNA concentration and purity were measured with a Nanophotometer (P-class, Implen, Germany). A total RNA of 2 μg was reverse transcribed using the PrimeScript™ II 1st Strand cDNA Synthesis Kit (TaKaRa, Japan). The concentration and purity of the cDNA were measured with a Nanophotometer (P-class, Implen, Germany). The qRT-PCR was performed on an ABI 7500TM Real-Time PCR System (Applied Biosystems, CA, USA). Each qPCR reaction was carried out in triplicate and consisted of 5 μL 2 × TB Green Premix Ex Taq II, 0.4 μL of each primer, 0.2 μL 50 × ROX Reference Dye, 1 μL of cDNA template, and 3 μL of ddH_2O. The PCR procedures for the amplification of *nap*A, *nir*S, *nos*Z, *hzs*B, *sqr* and *soxb* genes were described in detail in the Supplementary material (Table S4). The efficiencies of the real-time PCR assays were

over 95 % and the r^2 values were 0.99.

CRediT authorship contribution statement

Mengjia Zhan: Writing – original draft, Data curation, Conceptualization. **Wei Zeng:** Writing – review & editing, Funding acquisition. **Xiaojing Hao:** Methodology. **Haohao Miao:** Investigation. **Yao Lu:** Validation. **Wenzhuo Jiang:** Project administration. **Qingan Meng:** Visualization. **Qingteng Gong:** Formal analysis.

Declaration of competing interest

The authors declare that they have no known competing financial interests or personal relationships that could have appeared to influence the work reported in this paper.

Data availability

No data was used for the research described in the article

Acknowledgments

This research was supported by the National Key Research and Development Programme of China (2021YFC3200601) and the National Natural Science Foundation of China (52070004).

Supplementary materials

Supplementary material associated with this article can be found, in the online version, at doi:10.1016/j.wroa.2024.100257.

References

American Public Health Association (APHA), American Water Works Association (AWWA), Water Environment Federation (AEF), 2005. Standard Methods for the Examination of Water and Wastewater, twenty-first ed. Washington, DC, USA.

Ali, M., Rathnayake, R.M.L.D., Zhang, L., Ishii, S., Kindaichi, T., Satoh, H., Toyoda, S., Yoshida, N., Okabe, S., 2016. Source identification of nitrous oxide emission pathways from a single-stage nitritation-anammox granular reactor. Water Res. (Oxford) 102 (C), 147–157.

APHA, 2012. Standard Methods for the Examination of Water and Wastewater.

Brunet, R.C., GarciaGil, L.J., 1996. Sulfide-induced dissimilatory nitrate reduction to ammonia in anaerobic freshwater sediments. Fems Microbiol. Ecol. 21 (2), 131–138.

Bunse, P., Orschler, L., Agrawal, S., Lackner, S., 2020. Membrane aerated biofilm reactors for mainstream partial nitritation/anammox: experiences using real municipal wastewater. Water Res. X 9, 100066.

Cao, S., Wang, S., Peng, Y., Wu, C., Du, R., Gong, L., Ma, B., 2013. Achieving partial denitrification with sludge fermentation liquid as carbon source: the effect of seeding sludge. Bioresour. Technol. 149, 570–574.

Chen, C., Shao, B., Zhang, R.C., Xu, X.J., Zhou, X., Yuan, Y., Ren, N.Q., Lee, D.J., 2018. Mitigating adverse impacts of varying sulfide/nitrate ratios on denitrifying sulfide removal process performance. Bioresour. Technol. 267, 782–788.

Chen, H., Zeng, L., Wang, D., Zhou, Y., Yang, X., 2020. Recent advances in nitrous oxide production and mitigation in wastewater treatment. Water Res. (Oxford) 184, 116168.

Deng, Y.F., Wu, D., Huang, H., Cui, Y.X., van Loosdrecht, M., Chen, G.H., 2021. Exploration and verification of the feasibility of sulfide-driven partial denitrification coupled with anammox for wastewater treatment. Water Res. 193, 116905.

Derwis, D., Al-Hazmi, H.E., Majtacz, J., Kowal, P., Ciesielski, S., Mąkinia, J., 2024. The role of the combined nitrogen-sulfur-carbon cycles for efficient performance of anammox-based systems. Sci. Total Environ. 917, 170477.

Dolejs, P., Paclík, L., Maca, J., Pokorna, D., Zabranska, J., Bartacek, J., 2015. Effect of S/N ratio on sulfide removal by autotrophic denitrification. Appl. Microbiol. Biotechnol. 99 (5), 2383–2392.

Du, R., Cao, S.B., Jin, R.C., Li, X.C., Fan, J.R., Peng, Y.Z., 2022. Beyond an applicable rate in low-strength wastewater treatment by anammox: motivated labor at an extremely short hydraulic retention time. Environ. Sci. Technol. 56 (12), 8650–8662.

Du, R., Liu, Q.T., Li, C., Li, X.C., Cao, S.B., Peng, Y.Z., 2023. Spatiotemporal assembly and immigration of heterotrophic and anammox bacteria allow a robust synergy for high-rate nitrogen removal. Environ. Sci. Technol. 57 (24), 9075–9085.

Fortune, J., van de Kamp, J., Holmes, B., Bodrossy, L., Gibb, K., Kaestli, M., 2024. Dynamics of nitrogen genes in intertidal sediments of Darwin Harbour and their connection to N-biogeochemistry. Mar. Environ. Res. 198, 106500.

Fu, K., Kang, J., Zhao, J., Bian, Y., Li, X., Yang, W., Li, Z., 2023. Efficient nitrite accumulation in partial sulfide autotrophic denitrification (PSAD) system: insights of S/N ratio, pH and temperature. Environ. Technol. 1–18.

Huang, Y., Song, B., Zhang, Q., Park, Y., Wilson, S.J., Wilson, S.J., Tobias, C.R., An, S., 2024. Seawater intrusion effects on nitrogen cycling in the regulated Nakdong River Estuary, South Korea. Front. Mar. Sci. 11, 1369421.

Huo, P., Chen, X., Yang, L., Wei, W., Ni, B., 2022. Modeling of sulfur-driven autotrophic denitrification coupled with anammox process. Bioresour. Technol. 349, 126887.

Jones, C.M., Stres, B., Rosenquist, M., Hallin, S., 2008. Phylogenetic analysis of nitrite, nitric oxide, and nitrous oxide respiratory enzymes reveal a complex evolutionary history for denitrification. Mol. Biol. Evol. 25 (9), 1955–1966.

Joss, A., Salzgeber, D., Eugster, J., Konig, R., Rottermann, K., Burger, S., Fabijan, P., Leumann, S., Mohn, J., Siegrist, H., 2009. Full-scale nitrogen removal from digester liquid with partial nitritation and anammox in one SBR. Environ. Sci. Technol. 43 (14), 5301–5306.

Kalyuzhnyi, S., Gladchenko, M., Mulder, A., Versprille, B., 2006. DEAMOX—New biological nitrogen removal process based on anaerobic ammonia oxidation coupled to sulphide-driven conversion of nitrate into nitrite. Water Res. (Oxford) 40 (19), 3637–3645.

Kumar, M., Lin, J.G., 2010. Co-existence of anammox and denitrification for simultaneous nitrogen and carbon removal—Strategies and issues. J. Hazard. Mater. 178 (1–3), 1–9.

Kuypers, M.M.M., Marchant, H.K., Kartal, B., 2018. The microbial nitrogen-cycling network. Nat. Rev. Microbiol. 16 (5), 263–276.

Lee, D., Wong, B., 2014. Denitrifying sulfide removal by enriched microbial consortium: kinetic diagram. Bioresour. Technol. 164, 386–393.

Liu, C., Li, W., Li, X., Zhao, D., Ma, B., Wang, Y., Liu, F., Lee, D.J., 2017. Nitrite accumulation in continuous-flow partial autotrophic denitrification reactor using sulfide as electron donor. Bioresour. Technol. 243, 1237–1240.

Liu, Q., Li, C., Fan, J., Peng, Y., Du, R., 2023. Evaluation of sludge anaerobic fermentation driving partial denitrification capability: in view of kinetics and metagenomic mechanisms. Sci. Total Environ. 884, 163581.

Lu, H., Huang, H., Yang, W., Mackey, H.R., Khanal, S.K., Wu, D., Chen, G., 2018. Elucidating the stimulatory and inhibitory effects of dissolved sulfide on sulfur-oxidizing bacteria (SOB) driven autotrophic denitrification. Water Res. (Oxford) 133, 165–172.

Luo, J., Lin, W., Guo, Y., 2011. Functional genes-based analysis of sulfur-oxidizing bacteria community in sulfide removing bioreactor. Appl. Microbiol. Biotechnol. 90 (2), 769–778.

Martínez-Santos, M., Lanzén, A., Unda-Calvo, J., Martín, I., Garbisu, C., Ruiz-Romera, E., 2018. Treated and untreated wastewater effluents alter river sediment bacterial communities involved in nitrogen and sulphur cycling. Sci. Total Environ. 633, 1051–1061.

Polizzi, C., Gabriel, D., Munz, G., 2022. Successful sulphide-driven partial denitrification: efficiency, stability and resilience in SRT-controlled conditions. Chemosphere (Oxford) 295, 133936.

Qian, J., Zhang, M., Wu, Y., Niu, J., Chang, X., Yao, H., Hu, S., Pei, X., 2018. A feasibility study on biological nitrogen removal (BNR) via integrated thiosulfate-driven denitratation with anammox. Chemosphere 208, 793–799.

Qin, Y., Wu, C., Chen, B., Ren, J., Chen, L., 2019. Short term performance and microbial community of a sulfide-based denitrification and anammox coupling system at different N/S ratios. Bioresour. Technol. 294, 122130.

Reyes-Avila, J., Razo-Flores, E., Gomez, J., 2004. Simultaneous biological removal of nitrogen, carbon and sulfur by denitrification. Water Res. (Oxford) 38 (14), 3313–3321.

Seth, R., Prasad, D., Henry, J.G., 1995. Bioleaching of metals from sewage sludge: elemental sulfur recovery. J. Environ. Eng. (New York) 121 (7), 543–544.

Shi, M., Lv, C., Wu, P., Zhang, D., Li, X., Huang, Y., Yuan, Y., 2024. Effect of S/N ratio on operation characteristics and microbial community of double short-cut sulfur autotrophic denitrification system. J. Water Process. Eng. 59, 105025.

Strous, M., Kuenen, J.G., Jetten, M.S.M., 1999. Key physiology of anaerobic ammonium oxidation. Appl. Environ. Microbiol. 65 (7), 3248–3250.

Suenaga, T., Ota, T., Oba, K., Usui, K., Sako, T., Hori, T., Riya, S., Hosomi, M., Chandran, K., Lackner, S., Smets, B.F., Terada, A., 2021. Combination of 15N tracer and microbial analyses discloses N_2O sink potential of the anammox community. Environ. Sci. Technol. 55 (13), 9231–9242.

van Niftrik, L., Jetten, M.S., 2012. Anaerobic ammonium-oxidizing bacteria: unique microorganisms with exceptional properties. Microbiol. Mol. Biol. Rev. 76 (3), 585–596.

Wu, C., Qin, Y., Yang, L., Liu, Z., Chen, B., Chen, L., 2020. Effects of loading rates and N/S ratios in the sulfide-dependent autotrophic denitrification (SDAD) and anammox coupling system. Bioresour. Technol. 316, 123969.

Wu, P., Chen, J., Garlapati, V.K., Zhang, X., Wani Victor Jenario, F., Li, X., Liu, W., Chen, C., Aminabhavi, T.M., Zhang, X., 2022a. Novel insights into anammox-based processes: a critical review. Chem. Eng. J. (Lausanne, Switzerland: 1996) 444, 136534.

Wu, Y., Wan, Y., Tian, L., Liu, S., Pan, Y., Zhu, X., Han, Y., Li, N., Wang, X., 2022b. Bioelectrochemical partial denitrification coupled with anammox for autotrophic nitrogen removal. Chem. Eng. J. (Lausanne, Switzerland: 1996) 434, 134667.

Xu, G., Yin, F., Chen, S., Xu, Y., Yu, H., 2016. Mathematical modeling of autotrophic denitrification (AD) process with sulphide as electron donor. Water Res. (Oxford) 91, 225–234.

Xu, X., Chen, C., Wang, A., Guo, W., Zhou, X., Lee, D.J., Ren, N., Chang, J.S., 2014. Simultaneous removal of sulfide, nitrate and acetate under denitrifying sulfide

removal condition: modeling and experimental validation. J. Hazard. Mater. 264, 16–24.
Zhan, M., Zeng, W., Wu, C., Chen, G., Meng, Q., Hao, X., Peng, Y., 2024. Impact of organic carbon on sulfide-driven autotrophic denitrification: insights from isotope fractionation and functional genes. Water Res. (Oxford) 255, 121507.
Zhang, Q., Yang, Y., Zhang, X., Liu, F., Wang, G., 2022. Carbon neutral and techno-economic analysis for sewage treatment plants. Environ. Technol. Innov. 26, 102302.